EPSC Abstracts
Vol. 13, EPSC-DPS2019-118-1, 2019
EPSC-DPS Joint Meeting 2019

EPSC
EPSC-DPS Joint Meeting 2019
15–20 September 2019 | Geneva, Switzerland

An empirical model of Energetic Neutral Atom emission from the heliosphere – Implications for future heliospheric missions at large heliocentric distances

André Galli (1), Peter Wurz (1), Horst Fichtner (2), Yoshifumi Futaana (3), and Stas Barabash (3)
(1) Physics Institute, University of Bern, Bern, Switzerland (andre.galli@space.unibe.ch), (2) Ruhr University, Bochum, Germany, (3) IRF Swedish Institute of Space Physics, Kiruna, Sweden

Abstract

In this study, we present a simple empirical model of Energetic Neutral Atoms (ENA) from the heliosphere and derive basic requirements for ENA instrumentation onboard a spacecraft headed for heliocentric distances beyond Earth. We consider the energy range of heliospheric ENAs from 10 eV to 100 keV because each part of the energy spectrum has its own merit for heliospheric science.

1. Introduction

Several concepts for heliospheric missions operating at heliocentric distances far beyond Earth orbit are currently investigated by the scientific community. The mission concept of the Interstellar Probe, e.g., aims at reaching a distance of 1000 au away from the Sun within this century [11], far beyond the heliopause located at roughly 100-200 au [13]. This would, among many other scientific breakthroughs, allow the coming generation to obtain a global view of our heliosphere interacting with the interstellar medium by measuring the Energetic Neutral Atoms (ENAs) originating from the various plasma regions.

An ENA is created when a fast ion exchanges its charge with an ambient neutral atom. The resulting ENA leaves the source region on a straight trajectory, no longer influenced by electromagnetic fields. This allows an ENA camera to image the ion distribution of remote plasma regions. We therefore integrated the existing measurements of ENAs from the heliosphere into a simple empirical model to predict global ENA intensity maps for an observer at any heliocentric distance.

2. Our empirical ENA model

The fundamental ENA equation describes the differential intensity of ENAs at a given energy E as a line-of-sight (LOS) integral of the local proton intensity j_p multiplied by the neutral hydrogen density n_H, and the energy-dependent charge-exchange cross-section $\sigma(E)$:

$$j_{ENA} = \int_{\mathrm{LOS}} dl \, (j_p(E) \, n_H \, \sigma(E)) \qquad (1)$$

We only consider hydrogen ENAs in this study, assuming a constant n_H = 0.1 cm^{-3} inside the heliopause [15]. We use the $\sigma(E)$ for $H^+ + H \rightarrow H^* + H^+$ compiled by [1] and include loss processes due to the re-ionization of ENAs outside the heliopause. We distinguish three plasma regions as the places of origin for heliospheric ENAs: supersonic solar wind and pick-up ions inside the termination shock, shocked solar wind of the inner heliosheath, and the outer heliosheath. We scale the proton intensities j_p in such a way as to reproduce the heliospheric ENA measurements available so far (see Fig. 1). We further assume that the globally distributed heliospheric ENA flux apart from the IBEX Ribbon and the INCA Belt derives from the inner heliosheath [4] and that the IBEX Ribbon is caused by solar wind ENAs that leave the heliopause before being ionized and neutralized again outside the heliopause (so-called secondary ENAs, see [10, 17], e.g.). The proper motion of the spacecraft and plasma cooling in the heliosheath [15] can be taken into account. The true shape of the heliopause remains one of the open questions [13, 2, 16] to be resolved by a heliospheric probe at large heliocentric distances. We examined three shapes so far (a small ellipsoid, a large ellipsoid, and the cylindrical Parker shape [12, 14]), but others can easily be implemented.

3. Model results

Since our model is computationally not demanding, we can rapidly generate ENA maps from any vantage point inside or outside the heliosphere for a wide va-

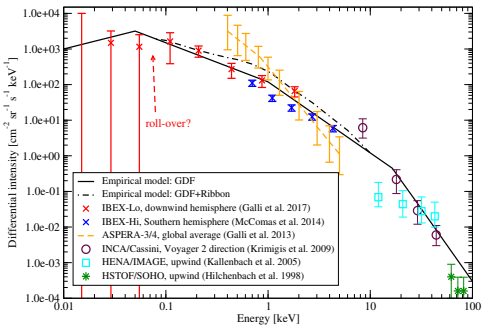

Figure 1: Energy spectra of heliospheric ENAs. The spectra assumed for the empirical model are plotted as black solid (globally distributed flux) and dashed-dotted line (IBEX Ribbon ENAs added), symbols denote observations (the HENA/IMAGE measurements are to be interpreted as upper limits [7]).

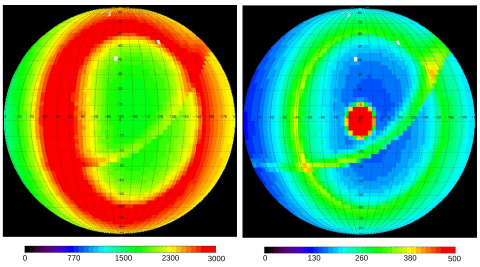

Figure 2: ENA map predictions for an observer in the inner heliosheath at 120 au heliocentric distance for ENA energies of 0.1 keV (left) and 1 keV (right) in units of cm^{-2} sr^{-1} s^{-1} keV^{-1}. The Sun is in the centre of the hemispherical maps.

riety of parameters and heliospheric shapes. Figure 2 shows two ENA maps for energies 100 eV and 1 keV predicted for a spacecraft in the ecliptic plane in the flank of the heliosheath (perpendicular to the inflow direction of the interstellar matter) at 120 au distance, looking back to the Sun. The IBEX Ribbon and the neutralized solar wind are most conspicuous at 1 keV (right panel), the region inside the termination shock shows up as an ENA cavity in all ENA energies. The heliopause shape in Fig. 2 is the small ellipsoid.

4. Implications for ENA cameras

From our model, general recommendation about ENA instrumentation (angular resolution, sensitivity etc.) will be derived. All energies from 10 eV to 100 keV have their own merits for heliospheric science. This implies two or three different ENA instruments for a future mission.

For a spacecraft orbiting the Sun, the heliocentric distance should be at least 3 au to better constrain the nature of the IBEX Ribbon ENAs via parallax effects [17]. For an interstellar probe, a radial trajectory through the flank regions of the heliosphere is preferable to a straight upwind or downwind trajectory.

References

[1] Barnett, C.F.: "Collisions of H, H_2, He and Li Atoms and Ions with Atoms and Molecules, Atomic Data for Fusion, Vol. 1", Oak Ridge National Laboratory, 1990.

[2] Dialynas, K., Krimigis, S.M., Mitchell, D.G., Decker, R.B., and Roelof, E.C.: Nature Astronomy, 1, 115, 2017.

[3] Galli, A., et al.: Astrophys. Jour., 775, 24, 2013.

[4] Galli, A., et al.: Astrophys. Jour., 821, 107, 2016.

[5] Galli, A., et al.: Astrophys. Jour., 851, 2, 2017.

[6] Hilchenbach, M., et al.: Astrophys. Jour., 503, 916, 1998.

[7] Kallenbach, R., Hilchenbach, M., Chalov, S.V., Le Roux, J. A., and Bamert, K.: Astronomy & Astrophysics, 439, 1, 2005.

[8] Krimigis, S.M., et al.: Science, 326, 971, 2009.

[9] McComas, D.J., et al.: Astrophys. Jour. Sup. Ser., 213, 20, 2014.

[10] McComas, D.J., et al.: Astrophys. Jour. Sup. Ser., 229, 41, 2017.

[11] McNutt, R.L., et al.: "Near-Term Interstellar Probe: First Step". Paper presented at the 69th International Astronautical Congress, Bremen, Germany, 2018.

[12] Parker, E.N.: Astrophys. Jour., 134, 20, 1961.

[13] Pogorelov, N.V., et al.: Sp. Sci. Rev., 212, 193-248, 2017.

[14] Röken, C., Kleimann, J., and Fichtner, H.: Astrophys. Jour., 805, 173, 2015.

[15] Schwadron, N.A., et al.: Astrophys. Jour., 731, 56, 2011.

[16] Schwadron, N.A., and Bzowski, M.: Astrophys. Jour., 862, 11, 2018.

[17] Swaczyna, P., et al.: Astrophys. Jour., 854, 2, 2018.